Sheffield Hallam University

Dilatational viscosity of dilute particle-laden fluid interface at different contact angles

LISHCHUK, Sergey <http://orcid.org/0000-0002-9989-765X>

Available from Sheffield Hallam University Research Archive (SHURA) at:

https://shura.shu.ac.uk/14203/

This document is the Published Version [VoR]

Citation:

LISHCHUK, Sergey (2016). Dilatational viscosity of dilute particle-laden fluid interface at different contact angles. Physical Review E (PRE), 94 (6), 063111. [Article]

Copyright and re-use policy

See http://shura.shu.ac.uk/information.html

Sheffield Hallam University Research Archive
http://shura.shu.ac.uk

Dilatational viscosity of dilute particle-laden fluid interface at different contact angles

Sergey V. Lishchuk
Materials and Engineering Research Institute, Sheffield Hallam University, Sheffield, United Kingdom
(Received 16 June 2016; published 22 December 2016)

We consider a solid spherical particle adsorbed at a flat interface between two immiscible fluids and having arbitrary contact angle at the triple contact line. We derive analytically the flow field corresponding to dilatational surface flow in the case of a large ratio of dynamic shear viscosities of two fluids. Considering a dilute assembly of such particles we calculate numerically the dependence on the contact angle of the effective surface dilatational viscosity particle-laden fluid interface. The effective surface dilatational viscosity is proportional to the size and surface concentration of particles and monotonically increases with the increase in protrusion of particles into the fluid with larger shear viscosity.

DOI: 10.1103/PhysRevE.94.063111

I. INTRODUCTION

The behavior of small particles adsorbed at interfaces between two fluids continues to be an area of great interest from an academic point of view as well as for its importance in many technological and industrial applications. The capability of the colloidal particles trapped at fluid interfaces to stabilize emulsions has applications in many industrial sectors, such as food processing [1], petroleum industry [2], biomedicine [3], etc.

The rheological properties of particle-laden fluid interfaces are known to be one of the key factors which influence stability of particle-laden emulsions and foams [1,4,5]. Better understanding of the rheological properties can help to enhance the stability of emulsions and foams and facilitate their use in fabrication of advanced materials, the examples of which are colloidosomes [6,7], armored bubbles [8,9], liquid marbles [10,11], bijels [12], and porous solids [13]. The study of the rheology of particle-laden fluid interfaces can provide new insight into their structure and properties [4,5].

Generally, particle-laden fluid interfaces are viscoelastic [5]. It is possible to separate viscous and elastic contributions to the surface stress by using appropriate constitutive equations [14]. For isotropic interfaces the viscous contribution is well described by a Boussinesq-Scriven model with surface shear and dilatational viscosities as the material properties [15,16]. In particular, isotropic change in the surface area results in a purely dilatational surface flow with the surface velocity field

$$\mathbf{v}_s = \alpha \mathbf{r}, \tag{1}$$

where α is the dilatation rate. The corresponding rate-of-strain tensor is isotropic,

$$\mathsf{S} = \alpha \mathsf{I}_s, \tag{2}$$

where I_s is the surface unit tensor. In this case the viscous contribution to the surface stress tensor,

$$\boldsymbol{\sigma}_v = \zeta_s \mathsf{S}, \tag{3}$$

contains a single material parameter, dilatational viscosity ζ_s. Note that ζ_s is the average, *effective* viscosity, which has sense on a large length scale where we can regard particle-laden interface as continuous.

In the case of a 90° contact angle, dilatational viscosity can be calculated analytically in the limits of low and high surface concentrations of particles. The origin of excess dissipation in particle-laden interfaces lies in modification by the particles of the flow in the bulk fluids that surround the interface. In the case of low concentration of the adsorbed particles the interaction between particles can be neglected and the effective dilatational viscosity is given by formula [17]

$$\zeta_s = 5(\eta_1 + \eta_2) R \phi \quad \text{(for small } \phi\text{)}, \tag{4}$$

where η_1 and η_2 are shear viscosities of the surrounding bulk fluids, R is the radius of the adsorbed particles, and

$$\phi = \frac{\pi R^2 N}{A} \tag{5}$$

is the surface concentration of the particles, where N is the number of particles in surface area A. In the opposite limit of high particle concentration the effective dilatational viscosity can be derived on the base of the facts that (i) highly concentrated particle arrays in a plane form a hexagonal structure and (ii) the dominant contribution to the viscous dissipation rate arises in the thin gaps between neighboring particles. The result is [18]

$$\zeta_s = \frac{3\sqrt{3}\pi(\eta_1 + \eta_2)R}{16(\sqrt{\phi_m/\phi} - 1)} \quad \text{(for large } \phi\text{)}, \tag{6}$$

where

$$\phi_m = \frac{\pi}{2\sqrt{3}} \tag{7}$$

is the maximum packing density of circles in the plane. The results (4) and (6) can be used as a starting approximation for more complicated (and common) systems in which the interparticle interactions of different nature cannot be neglected.

The above results were derived for the case of 90° contact angle. On one hand, this allows us to exploiting the symmetry of the system, making the derivation easier. On the other hand, in the most common systems particles form arbitrary contact angles with the fluid interface due to different nature of fluids at both sides of the interface. Contact angle can be controlled, for example, by modifying chemical composition of the particle surfaces [19] or fluid phase [20]. This, in turn, allows controlling particle packing density [21], their

 ©2016 American Physical Society

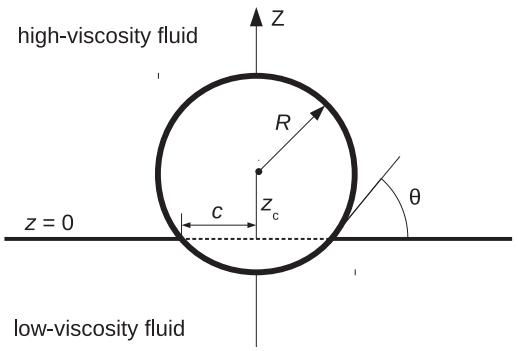

FIG. 1. The geometry of the system.

detachment energy [21,22], and the type of particle-stabilized emulsions (e.g., air-in-water or water-in-air [19], oil-in-water or water-in-oil [20]), as predicted Finkle and others [23]. Contact angle influences drag and diffusion coefficients of the particles at fluid interfaces [24–26] as well as their electrostatic properties [27].

This paper extends the result for the effective dilatational viscosity of particle-laden fluid interfaces in the limit of low surface concentration of particles, Eq. (4), to arbitrary contact angles. At that, we simplify the analysis by neglecting the viscosity of one of the fluids because high ratio of dynamics shear viscosities is commonly encountered in practice, for example, water-air or oil-water interfaces typically have shear viscosity contrast of two orders of magnitude.

The paper is organized as follows. After formulating the model (Sec. II) and writing the corresponding general expression for the dissipation energy (Sec. III), we proceed to derivation of the analytical expression for the velocity field (Sec. IV). Numerical integration of the velocity then provides the distribution of pressure at the surface of the particle (Sec. V) and the effective dilatational viscosity (Sec. VI), which is the main result of this paper. The dependence of the effective dilatational viscosity on the contact angle is given by Eq. (66), tabulated in Table I, and illustrated graphically in Fig. 3.

II. MODEL

We consider a system of identical rigid spherical particles of radius R adsorbed at the flat interface between two incompressible fluids. We assume the particles are far enough from each other so their interactions of any nature can be neglected.

We suppose a macroscopically thin fluid interface is located at $z = 0$ and separates a high viscosity fluid ($z > 0$) with dynamic viscosity η and a low viscosity fluid ($z < 0$) which viscosity we shall neglect. We suppose surface tension γ to be high enough so flow and gravity do not distort the flat shape of the interface. We assume that the interfacial tensions favor a contact angle θ as shown in Fig. 1. This definition of θ agrees with the commonly accepted one for air-water interface but is supplementary to commonly accepted definition for oil-water interface. For consistency, we will use the same definition, shown in Fig. 1, for all cases. Then the vertical position of the particles' centers is given by

$$z_c = R\sin\theta, \tag{8}$$

the protrusion of the particles into the large-viscosity fluid is $R + z_c$, and the radius of the triple contact circle is

$$c = R\cos\theta. \tag{9}$$

We shall accept Eq. (5) as the definition of the surface concentration of particles, although it no longer has meaning of the fraction of the surface area taken by particles in the cases when the contact angle differs from 90°.

In small-Reynolds-number flow the velocity $\mathbf{v}$ and pressure p of high-viscosity fluid satisfy the Stokes equation

$$\mu\nabla^2\mathbf{v} = \nabla p \tag{10}$$

and the continuity equation

$$\boldsymbol{\nabla}\cdot\mathbf{v} = 0. \tag{11}$$

We assume no-slip boundary condition at the surface of the particle,

$$\mathbf{v} = \mathbf{0}. \tag{12}$$

Since the position of the fluid interface remains constant, the kinematic boundary condition at the fluid interface is

$$\mathbf{v}\cdot\mathbf{n} = 0, \tag{13}$$

where $\mathbf{n}$ is the unit vector normal to the interface. Since we neglect the motion of the low-viscosity fluid, the dynamic boundary condition can be written in the following form:

$$\frac{\partial\mathbf{v}_t}{\partial z} = \mathbf{0}, \tag{14}$$

where $\mathbf{v}_t$ is the component of the velocity tangential to the interface.

We subject the system to the flow which in the absence of the particles would be written in cylindrical coordinates (r,ϕ,z) as

$$v_r^{(0)} = \alpha r, \quad v_\phi^{(0)} = 0, \quad v_z^{(0)} = -2\alpha z \tag{15}$$

and corresponds to the dilatational surface flow given by Eq. (1).

III. ENERGY DISSIPATION

Particle-laden fluid interface can be viewed on a macroscopic scale as continuous, characterized by some effective properties. Let us consider such "macroscopic" version of the model described in the previous section. Then, instead of particles straddling the interface, we will have a homogeneous fluid interface characterized, in particular, by some effective dilatation viscosity ζ_s. Consider a large sphere located somewhere at the interface and having a volume V_0. The additional contribution to the energy dissipation rate which arises due to the dilatational flow at the interface is [17,18]

$$\dot{E} = \zeta_s(\mathrm{Tr}\,\mathsf{S})^2 A_s, \tag{16}$$

where A_s is the area of the fluid interface contained within volume V_0. Substituting $(\mathrm{Tr}\,\mathsf{S})^2 = 4\alpha^2$ in accordance with Eq. (2), we obtain

$$\dot{E} = 4\zeta_s\alpha^2 A_s. \tag{17}$$

We can use Eq. (17) as the definition of the effective dilatational viscosity and determine its value by calculating the contribution to the energy dissipation rate of the particle-laden

interface due to the presence of the particles. This approach was pioneered by Einstein, who used it to determine the effective shear viscosity of dilute suspensions [28]. Similar approach can be used to define effective surface shear viscosity of particle-laden fluid interfaces [17,29].

The expression for the rate of energy dissipation in particle-laden flows can be cast in a form of an integral over the surface of the particles A_p provided the integral

$$\boldsymbol{\alpha}\cdot\int_V\left[\left(\frac{\partial\boldsymbol{\sigma}^{(1)}}{\partial\mathbf{r}}\right)\mathbf{r}+\boldsymbol{\sigma}^{(1)}\right]dV \tag{18}$$

over the volume V occupied by fluid inside A_s equals zero [30,31]. In Eq. (18), $\boldsymbol{\alpha}$ is the rate-of-strain tensor corresponding to the fluid flow unperturbed by particles [in our case it is given by Eq. (15)], and

$$\boldsymbol{\sigma}^{(1)}=-p^{(1)}\mathbf{I}+\eta[\nabla\mathbf{v}^{(1)}+(\nabla\mathbf{v}^{(1)})^{\mathrm{T}}] \tag{19}$$

is the contribution to the stress tensor due to the presence of the particles. The value of the shear viscosity η generally differs in different fluid components. This results in the discontinuity in the stress field at the interface. Nevertheless, it is straightforward to check that the integral (18) indeed equals zero in the case if identical particles are adsorbed at the interface between two fluids provided there is no extra dissipation of energy at the interface (for example, due to adsorbed surfactants). Then the expression for the rate of energy dissipation can be written as [17,29]

$$\dot{E}=N\int_{A_p}[(\boldsymbol{\alpha}\cdot\mathbf{r})\cdot(\boldsymbol{\sigma}^{(1)}\cdot\mathbf{n})-2\eta(\boldsymbol{\alpha}:\mathbf{v}^{(1)}\mathbf{n})]dA, \tag{20}$$

where N is the number of particles adsorbed at the interface of area A_s.

The velocity and pressure fields can be represented as sums of unperturbed contributions $\mathbf{v}^{(0)}$, given by Eq. (15), and $p^{(0)}$, which is constant, and the perturbations due to particles, denoted by superscript (1):

$$\mathbf{v}=\mathbf{v}^{(0)}+\mathbf{v}^{(1)}, \tag{21}$$

$$p=p^{(0)}+p^{(1)}. \tag{22}$$

If the particles are far enough from each other, then the velocity and pressure fields can be determined as a solution to Stokes equations (10) and (11) for the flow with only one particle present, which is done in the following two sections. Then the effective dilatational viscosity is obtained by equating expressions (17) and (20):

$$\zeta_s=\frac{\phi}{4\pi R^2\alpha^2}\times\int_{A_p}[(\boldsymbol{\alpha}\cdot\mathbf{r})\cdot(\boldsymbol{\sigma}^{(1)}\cdot\mathbf{n})-2\eta(\boldsymbol{\alpha}:\mathbf{v}^{(1)}\mathbf{n})]dA. \tag{23}$$

IV. VELOCITY FIELD

This section presents the velocity field for the dilatational flow in the presence of a spherical particle adsorbed at a fluid interface, according to the model described in Sec. II. Without loss of generality, we will assume that the radius of the particle, R, is equal to 1. Our derivation is a modification of the derivation by El-Kareh and Secomb [32] with no-slip boundary condition at the solid wall replaced by the free-surface boundary condition at the fluid interface.

The velocity of an axially symmetric flow is expressed in terms of stream function Ψ as [32]

$$\mathbf{v}=\nabla\cdot\left(\frac{\Psi}{r}\mathbf{e}_\phi\right), \tag{24}$$

where cylindrical coordinate system (r,ϕ,z) is used. The stream function Ψ can be decomposed as

$$\Psi=\psi_0+\psi, \tag{25}$$

according to decomposition of velocity given by Eq. (21). The contribution which corresponds to the unperturbed flow with velocity $\mathbf{v}^{(0)}$ is

$$\psi_0=-\alpha r^2 z. \tag{26}$$

The general approach for solving Stokes equations in axially symmetric systems was formulated by El-Kareh and Secomb [32] and, in an alternative form, by Zabarankin and coauthors [33,34]. For the stream function contribution ψ, which corresponds to the disturbance velocity $\mathbf{v}^{(1)}$, we shall use the general solution in the form given by El-Kareh and Secomb [32], which tends to zero far from the particle:

$$\psi=2\,\mathrm{Re}\left\{\frac{1}{(\cosh\xi-\cos\eta)^{3/2}}\int_0^\infty\left[P_{i\tau-\frac{3}{2}}(\cosh\xi)-P_{i\tau+\frac{1}{2}}(\cosh\xi)\right][A(\tau)\cos[(i\tau-1)\eta]+B(\tau)\cos[(i\tau+1)\eta]+C(\tau)\sin[(i\tau-1)\eta]+D(\tau)\sin[(i\tau+1)\eta]]d\tau\right\}. \tag{27}$$

Here $P_\nu(z)$ are Legendre functions of the first kind [35,36].

In Eq. (27) the toroidal coordinate system (ξ,θ,ϕ) is used, in which both the surface of the particle and the fluid interface coincide with the coordinate surfaces [25,27,37,38]. In the meridional cross-section plane (r,z) toroidal coordinates (ξ,η) are introduced by [39,40]

$$r=\frac{c\sinh\xi}{\cosh\xi-\cos\eta},\quad z=\frac{c\sin\eta}{\cosh\xi-\cos\eta}, \tag{28}$$

where a metric parameter c is shown in Fig. 1. The azimuthal coordinate ϕ is common to both coordinate systems. The fluid interface corresponds to $\eta=0$, and the surface of the particle in contact with a viscous liquid ($z>0$) corresponds to a coordinate surface $\eta=\eta_0$, where $\eta_0=\arcsin c$. We can express the vertical position of the particle's center in terms of η_0 as $z_c=\cos\eta_0$. Note that the contribution (26) to the stream function corresponding to unperturbed flow is written

in toroidal coordinates as

$$\psi_0 = -\frac{\alpha c^3 \sin\eta \sinh^2\xi}{(\cosh\xi - \cos\eta)^3}. \tag{29}$$

The functions $A(\tau)$, $B(\tau)$, $C(\tau)$, and $D(\tau)$, which enter Eq. (27), can be determined by applying boundary conditions (12)–(14). Similarly to Ref. [32], we can set to zero the value of the stream function Ψ both at the surface of the particle and at the fluid interface because they form a single stream surface in accordance with the boundary conditions (12) and (13):

$$\Psi = 0 \quad \text{at } \eta = 0 \quad \text{and} \quad \eta = \eta_0. \tag{30}$$

The no-slip boundary condition at the surface of the particle, Eq. (12), also yields

$$\frac{\partial\Psi}{\partial\eta} = 0 \quad \text{at } \eta = \eta_0. \tag{31}$$

A dynamic boundary condition at the fluid interface, Eq. (14), is written in terms of Ψ as

$$\frac{\partial^2\Psi}{\partial\eta^2} = 0 \quad \text{at } \eta = 0. \tag{32}$$

Taking into account that the base flow (29) satisfies free-flow boundary conditions at the fluid interface, we can rewrite the above equations in terms of the disturbance stream function ψ as

$$\psi = 0, \quad \frac{\partial^2\psi}{\partial\eta^2} = 0 \quad \text{at } \eta = 0, \tag{33}$$

$$\psi = -\psi_0, \quad \frac{\partial\psi}{\partial\eta} = -\frac{\partial\psi_0}{\partial\eta} \quad \text{at } \eta = \eta_0. \tag{34}$$

Application of the boundary conditions at the fluid interface, Eq. (33), to Eq. (27) yields

$$A(\tau) = 0 \quad \text{and} \quad B(\tau) = 0. \tag{35}$$

With this, the stream function (27) can be rewritten in the form

$$\psi = \frac{2}{(\cosh\xi - \cos\eta)^{3/2}} \int_0^\infty R(\tau,\xi) k(\tau,\eta) d\tau \tag{36}$$

with

$$R(\tau,\xi) = i\left[P_{i\tau-\frac{3}{2}}(\cosh\xi) - P_{i\tau+\frac{1}{2}}(\cosh\xi)\right] \tag{37}$$

and

$$k(\tau,\eta) = E(\tau)\sin\eta\cosh(\eta\tau) + F(\tau)\cos\eta\sinh(\eta\tau), \tag{38}$$

where the functions $E(\tau)$ and $F(\tau)$ are determined by the boundary conditions at the surface of the particle.

Using the relations

$$(\cosh\xi - \cos\eta)^{\frac{3}{2}}\psi|_{\eta=\eta_0} = \int_0^\infty R(\tau,\xi) G_1(\tau) d\tau \tag{39}$$

and

$$\frac{\partial}{\partial\eta}[(\cosh\xi - \cos\eta)^{\frac{3}{2}}\psi]\Big|_{\eta=\eta_0} = \int_0^\infty R(\tau,\xi) G_2(\tau) d\tau, \tag{40}$$

where

$$G_1(\tau) = 2E(\tau)\sin\eta_0\cosh(\eta_0\tau) + 2F(\tau)\cos\eta_0\sinh(\eta_0\tau), \tag{41}$$

$$G_2(\tau) = 2E(\tau)[\cos\eta_0\cosh(\eta_0\tau) + \tau\sin\eta_0\sinh(\eta_0\tau)] - 2F(\tau)[\sin\eta_0\sinh(\eta_0\tau) - \tau\cos\eta_0\cosh(\eta_0\tau)], \tag{42}$$

the boundary conditions on the surface of the particle, Eq. (34), can be cast as

$$\int_0^\infty R(\tau,\xi) G_1(\tau) d\tau = -(\cosh\xi - \cos\eta)^{\frac{3}{2}}\psi_0\Big|_{\eta=\eta_0} \tag{43}$$

and

$$\int_0^\infty R(\tau,\xi) G_2(\tau) d\tau = -\frac{\partial}{\partial\eta}[(\cosh\xi - \cos\eta)^{\frac{3}{2}}\psi_0]\Big|_{\eta=\eta_0}. \tag{44}$$

The functions $E(\tau)$ and $F(\tau)$ are given by formulas

$$E(\tau) = \frac{[\sin\eta_0\sinh(\eta_0\tau) - \tau\cos\eta_0\cosh(\eta_0\tau)]G_1(\tau) + \cos\eta_0\sinh(\eta_0\tau)G_2(\tau)}{\sinh(2\eta_0\tau) - \tau\sin(2\eta_0)} \tag{45}$$

and

$$F(\tau) = \frac{[\cos\eta_0\cosh(\eta_0\tau) + \tau\sin\eta_0\sinh(\eta_0\tau)]G_1(\tau) - \sin\eta_0\cosh(\eta_0\tau)G_2(\tau)}{\sinh(2\eta_0\tau) - \tau\sin(2\eta_0)}, \tag{46}$$

where $G_1(\tau)$ and $G_2(\tau)$ satisfy Eqs. (43) and (44). In order to determine the explicit form of the functions $G_1(\tau)$ and $G_2(\tau)$ we substitute Eq. (29) for ψ_0 into Eqs. (43) and (44) to obtain

$$\int_0^\infty R(\tau,\xi) G_1(\tau) d\tau = \frac{\alpha c^3 \sinh^2\xi \sin\eta_0}{(\cosh\xi - \cos\eta_0)^{3/2}} \tag{47}$$

and

$$\int_0^\infty R(\tau,\xi) G_2(\tau) d\tau = \frac{\alpha c^3 \sinh^2\xi\cos\eta_0}{(\cosh\xi - \cos\eta_0)^{3/2}} - \frac{3\alpha c^3}{2}\frac{\sinh^2\xi\sin^2\eta_0}{(\cosh\xi - \cos\eta_0)^{5/2}}. \tag{48}$$

Applying operator $\sinh\xi(d/d\xi)$ to both sides of Mehler-Fock representations [41]

$$\frac{1}{(\cosh\xi-\cos\eta_0)^{1/2}}=\sqrt{2}\int_0^\infty \tanh(\pi\tau)P_{i\tau-\frac{1}{2}}(\cosh\xi)\times\frac{\cosh[(\pi-\eta_0)\tau]}{\sinh(\pi\tau)}d\tau \tag{49}$$

and

$$\frac{1}{(\cosh\xi-\cos\eta_0)^{3/2}}=\frac{2\sqrt{2}}{\sin\eta_0}\int_0^\infty \tau\tanh(\pi\tau)P_{i\tau-\frac{1}{2}}(\cosh\xi)\times\frac{\sinh[(\pi-\eta_0)\tau]}{\sinh(\pi\tau)}d\tau \tag{50}$$

and using the identity [32]

$$\sinh\xi\frac{dP_{i\tau-\frac{1}{2}}(\cosh\xi)}{d\xi}=-\frac{\tau^2+\frac{1}{4}}{2\tau}R(\tau,\xi), \tag{51}$$

we obtain the relations

$$\frac{\sinh^2\xi}{(\cosh\xi-\cos\eta_0)^{3/2}}=\sqrt{2}\int_0^\infty\left(\tau^2+\frac{1}{4}\right)\frac{\cosh[(\pi-\eta_0)\tau]}{\tau\cosh(\pi\tau)}R(\tau,\xi)d\tau \tag{52}$$

and

$$\frac{3\sinh^2\xi}{(\cosh\xi-\cos\eta_0)^{5/2}}=\frac{2\sqrt{2}}{\sin\eta_0}\int_0^\infty\left(\tau^2+\frac{1}{4}\right)\times\frac{\sinh[(\pi-\eta_0)\tau]}{\cosh(\pi\tau)}R(\tau,\xi)d\tau, \tag{53}$$

which together with Eqs. (47) and (48) yield

$$G_1(\tau)=\frac{\sqrt{2}\alpha c^3}{\tau\cosh(\pi\tau)}\left(\tau^2+\frac{1}{4}\right)\sin\eta_0\cosh[(\pi-\eta_0)\tau] \tag{54}$$

and

$$G_2(\tau)=\frac{\sqrt{2}\alpha c^3}{\tau\cosh(\pi\tau)}\left(\tau^2+\frac{1}{4}\right)\{\cos\eta_0\cosh[(\pi-\eta_0)\tau]-\tau\sin\eta_0\sinh[(\pi-\eta_0)\tau]\}. \tag{55}$$

As a result, the velocity field is given by Eq. (24), where the stream function Ψ, Eq. (25), is a sum of the base flow contribution ψ_0, given by Eq. (29), and the disturbance contribution ψ, given by the integral (36) with the integrand defined by Eqs (45), (46), (54), and (55). Figure 2 depicts stream lines of this flow at different contact angles.

V. PRESSURE ON PARTICLE SURFACE

The pressure distribution on the surface of a spherical particle with no-slip boundary condition was found by El-Kareh and Secomb [32] to satisfy the equation

$$\frac{1}{\mu}\left(\frac{\partial p}{\partial\xi}\right)_{\eta=\eta_0}=\frac{1}{c^3\sinh\xi}\left\{\frac{\partial}{\partial\eta}\left[(\cosh\xi-\cos\eta)^3\frac{\partial^2\Psi}{\partial\eta^2}\right]\right\}_{\eta=\eta_0}. \tag{56}$$

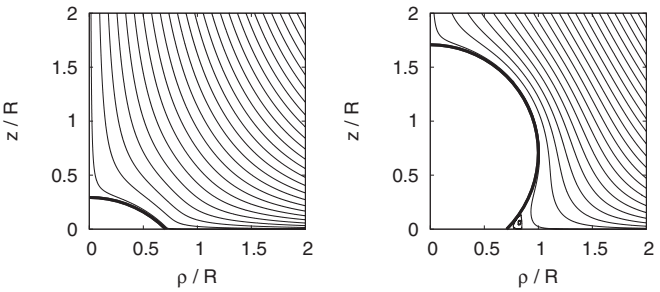

FIG. 2. Streamlines of the velocity field at different values of the contact angle: $\theta=135^\circ$ (left) and $\theta=45^\circ$ (right).

Substituting Eqs (25), (29), and (36) for stream function Ψ, we can write

$$\left(\frac{\partial p}{\partial\xi}\right)_{\eta=\eta_0}=\frac{\mu}{c^3}\frac{1}{\sinh\xi}\left\{(\cosh\xi-\cos\eta)^{3/2}\times\left[\frac{\partial^3 f}{\partial\eta^3}+2\int_0^\infty R(\tau,\xi)\frac{\partial^3 k}{\partial\eta^3}d\tau\right]-\frac{3}{2}(\cosh\xi-\cos\eta)^{1/2}\times\sin\eta\left[\frac{\partial^2 f}{\partial\eta^2}+2\int_0^\infty R(\tau,\xi)\frac{\partial^2 k}{\partial\eta^2}d\tau\right]\right\}_{\eta=\eta_0}, \tag{57}$$

where

$$f=(\cosh\xi-\cos\eta)^{3/2}\psi_0. \tag{58}$$

The pressure distribution on the surface of the particle can be found by integrating Eq. (57):

$$p(\xi)=p_0+\int_0^\xi\left(\frac{\partial p}{\partial\xi}\right)_{\eta=\eta_0}d\xi. \tag{59}$$

We shall neglect the integration constant p_0 because does not affect the calculated value of the effective dilatational viscosity ζ_s. This follows from the Stokes equation (10), which contains only gradient of pressure, and can also be directly verified by substituting in Eq. (23) the contribution $-p_0\mathbf{I}$ to the stress tensor. We shall therefore calculate pressure using formula

$$p(\xi)=\int_0^\xi\left(\frac{\partial p}{\partial\xi}\right)_{\eta=\eta_0}d\xi. \tag{60}$$

VI. DILATATIONAL VISCOSITY

In order to calculate dilatational viscosity we need to evaluate the integral in Eq. (23). It is convenient to split it in two parts corresponding to two terms in the integrand:

$$\int_{A_p}[(\boldsymbol{\alpha}\cdot\mathbf{r})\cdot(\boldsymbol{\sigma}^{(1)}\cdot\mathbf{n})-2\eta(\boldsymbol{\alpha}:\mathbf{v}^{(1)}\mathbf{n})]dA=\mathcal{I}_1+\mathcal{I}_2. \tag{61}$$

The second part, $\mathcal{I}_2$, can be integrated analytically:

$$\mathcal{I}_2\equiv\int_{A_p}[-2\eta(\boldsymbol{\alpha}:\mathbf{v}^{(1)}\mathbf{n})]dA=4\pi\eta\alpha^2(R+z_c)(R^2-z_c^2). \tag{62}$$

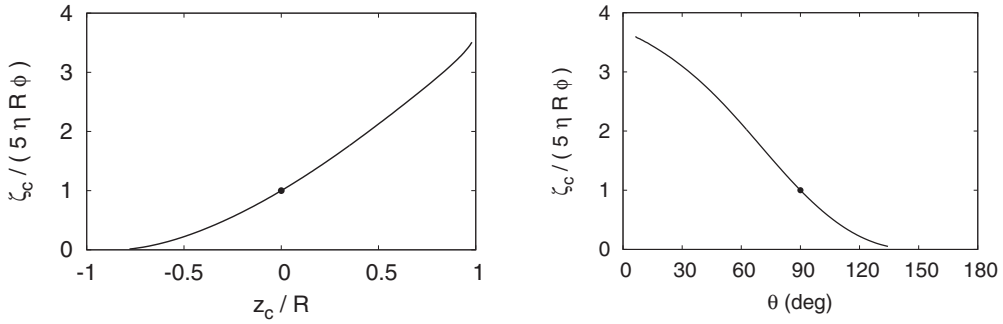

FIG. 3. Dependence of the dilatational viscosity on the vertical position of the particle's center z_c (left) and the contact angle θ (right). Solid circle corresponds to the case of 90° contact angle described by Eq. (4) with $\eta_1 = \eta$, $\eta_2 = 0$.

The first part,

$$\mathcal{I}_1 \equiv \int_{A_p} [(\boldsymbol{\alpha}\cdot\mathbf{r})\cdot(\boldsymbol{\sigma}^{(1)}\cdot\mathbf{n})]dA, \tag{63}$$

can be represented in form

$$\mathcal{I}_1 = \alpha\int_0^{(1+z_c)R}\left\{\eta\rho\left[4\rho\frac{\partial v_\rho}{\partial\rho} - (z+z_c)\frac{\partial v_\rho}{\partial z} - 2v_\rho\right]\right.$$
$$-2\eta\left[\rho(z+z_c)\frac{\partial v_z}{\partial\rho} + 2z(z-z_c)\frac{\partial v_z}{\partial z} - 2(z-z_c)v_z\right]$$
$$\left.+[2z(z-z_c)-\rho^2]p\right\}_{\rho=\sqrt{1-(z-z_c)^2}R} dz, \tag{64}$$

where the integrand is evaluated at the surface of the particle and can be calculated numerically using velocity given by Eqs. (24), (25), (29), (36), (45), (46), (54), and (55), and pressure given by Eqs. (60), (57), and (58). The effective dilatational viscosity is then calculated by formula

$$\zeta_s = \frac{\phi}{4\pi R^2\alpha^2}(\mathcal{I}_1+\mathcal{I}_2). \tag{65}$$

The final result can be represented in form

$$\zeta_s = 5\eta R\phi K(\theta), \tag{66}$$

where the dependence of ζ_s on the contact angle is described by the factor $K(\theta)$. In case of $\theta = 90°$ the viscosity is described by Eq. (4) with $\eta_2 = 0$, and therefore we have $K(\pi/2) = 1$ exactly. In order to obtain $K(\theta)$ for other values of the contact angle, the numerical integration of Eq. (64) was carried out using the algorithms implemented in the GNU Scientific Library [42]. At that, the function $R(\tau,\xi)$ was calculated using the software described in Ref. [43] for small values of ξ and by substituting the asymptotic expansion of the conical function [44] in Eq. (51) at large values of ξ.

The numerical results for $K(\theta)$ are presented in Fig. 3 and Table I. Increasing the protrusion of particles into the fluid with higher shear viscosity, z_c, leads to increase in the distortion of the base flow and, consequently, to increase in viscous dissipation of energy, which is manifested as a monotonic growth of the effective surface dilatational viscosity $\zeta_s(z_c)$.

The values $z_c > R$, not considered here, would correspond to a system in which the particles form a flat layer without contact with fluid interface. In the limit $z_c \to \infty$ the particles will be far from the interface. The dilatational viscosity of this hypothetical system can be calculated by setting equal shear viscosities of two bulk fluids, $\eta_1 = \eta_2$, in Eq. (4), leading to the value $K(z_c \to \infty) = 2$ which is less than the maximum value in Fig. 3. Thus the maximum dilatational viscosity corresponds to some value of z_c at which particles do not straddle the interface. This can be qualitatively explained by "screening" of the flow by the particles with large z_c, leading to the increased distortion of the velocity field in some volume "below" the particle (an example of such distortion can bee seen in Fig. 2, where a vortex appears at $\theta = 45°$, which can be considered an axisymmetric equivalent of Moffatt eddies [45]).

We conclude this section by summarizing the conditions of applicability of the results of this paper. It follows from the assumptions of the model that in order for the results to be valid the surface concentration of particles has to be small ($\phi \ll 1$), and the ratio of shear viscosities of both fluids has to be large ($\eta_1 \gg \eta_2$). Additionally, shear rate has to be small enough [29] to reduce the inertial effects,

$$\alpha \ll \frac{\eta}{\rho_f R^2} \tag{67}$$

(ρ_f is the fluid density) and to keep the interface flat,

$$\alpha \ll \frac{\gamma}{\eta R} \tag{68}$$

(γ is the surface tension). These are rather weak restrictions: For example, for a micron-sized particle at an air-water interface they require the shear rate to be small compared to $\sim 10^6$ s^{-1}, which is well satisfied in experiments.

TABLE I. Values of the function $K(\theta)$, defined by Eq. (66), at different values of θ.

Contact angle θ (°)	15	30	45	60	75	90	105	120	135
Dilatational viscosity factor $K(\theta)$	3.44	3.10	2.66	2.13	1.55	1.00	0.54	0.22	0.05

VII. CONCLUDING REMARKS

We have calculated the effective surface dilatational viscosity of an interface between two immiscible fluids having large viscosity contrast and decorated with a system of monodisperse solid spherical particles, favoring different contact angles at the triple contact line, in the limit of small surface concentration of particles. The effective surface dilatational viscosity is proportional to the size and surface concentration of the particles and monotonically increases with the increase in the protrusion of the particles into the fluid with higher shear viscosity, as depicted in Fig. 3. Experimental and computer simulation studies of dilatational rheology of particle-laden interfaces in the dilute regime can establish the limits of applicability of this result and, possibly, provide new insight into the mechanisms of viscous dissipation in such systems. The results can be used as a reference approximation for higher-concentrated systems in which the interparticle interactions cannot be neglected.

The derivation was carried in assumption that the viscosity of one of the fluids is small compared to another. This is the most common case in practice, exemplified by oil-water and water-air interfaces. The result can be extended to the case of comparable viscosities of two fluids by modifying the dynamic boundary condition (14). Such extension should be also applicable to the cases in which the larger part of the particle is in contact with the low-viscosity fluid so the disturbance of flow in the low-viscosity fluid is large compared to the high-viscosity fluid, making it necessary to take into account viscous dissipation in both fluids.

Considering the same system subjected to a different type of flow, which corresponds to the surface shear flow, should allow us to calculate the effective surface shear viscosity of dilute particle-laden interfaces at arbitrary contact angles using the similar method. The general method to deal with complications which arise due to break of the axial symmetry of the flow has been developed by Zabarankin and Krokhmal [34]. We may expect that the "screening" of the flow by particles, described in Sec. VI, would not appear in the case of the bulk fluid flow corresponding to surface shear flow, so surface shear viscosity would not increase as fast as dilatational viscosity with the increase in the protrusion of particles into the high-viscosity fluid.

[1] E. Dickinson, Curr. Opin. Colloid Interface Sci. **15**, 40 (2010).
[2] P. A. Kralchevsky, V. N. Paunov, I. B. Ivanov, and K. Nagayama, Oil Gas Sci. Tech. **59**, 511 (2004).
[3] S. Shilpi, A. Jain, Y. Gupta, and S. K. Jain, Crit. Rev. Ther. Drug Carrier Syst. **24**, 361 (2007).
[4] G. G. Fuller and J. Vermant, Ann. Rev. Chem. Biomol. Eng. **3**, 519 (2012).
[5] A. J. Mendoza, E. Guzmán, F. Martínez-Pedrero, H. Ritacco, R. G. Rubio, F. Ortega, V. M. Starov, and R. Miller, Adv. Colloid Interface Sci. **206**, 303 (2014).
[6] A. D. Dinsmore, M. F. Hsu, M. G. Nikolaides, M. Marquez, A. R. Bausch, and D. A. Weitz, Science **298**, 1006 (2002).
[7] P. Dommersnes, Z. Rozynek, A. Mikkelsen, R. Castberg, K. Kjerstad, K. Hersvik, and J. O. Fossum, Nat. Commun. **4**, 2066 (2013).
[8] A. B. Subramaniam, M. Abkarian, L. Mahadevan, and H. A. Stone, Nature **438**, 930 (2005).
[9] M. Cui, T. Emrick, and T. P. Russell, Science **342**, 460 (2013).
[10] P. Aussillous and D. Quéré, Nature **411**, 924 (2001).
[11] E. Bormashenko, Soft Matter **8**, 11018 (2012).
[12] M. E. Cates and P. S. Clegg, Soft Matter **4**, 2132 (2008).
[13] B. Neirinck, J. Fransaer, O. van der Biest, and J. Vleugels, Adv. Eng. Mater. **9**, 57 (2007).
[14] T. Verwijlen, L. Imperiali, and J. Vermant, Adv. Colloid Interface Sci. **206**, 428 (2014).
[15] L. E. Scriven, Chem. Eng. Sci. **12**, 98 (1960).
[16] R. Aris, *Vectors, Tensors, and the Basic Equations of Fluid Mechanics* (Dover, London, 1989).
[17] S. V. Lishchuk and I. Halliday, Phys. Rev. E **80**, 016306 (2009).
[18] S. V. Lishchuk, Phys. Rev. E **90**, 053005 (2014).
[19] B. P. Binks and R. Murakami, Nat. Mater. **5**, 865 (2006).
[20] M. Destribats, S. Gineste, E. Laurichesse, H. Tanner, F. Leal-Calderon, V. Héroguez, and V. Schmitt, Langmuir **30**, 9313 (2014).
[21] B. P. Binks, Curr. Opin. Colloid Interface Sci. **7**, 21 (2002).
[22] R. Ettelaie and S. V. Lishchuk, Soft Matter **11**, 4251 (2015).
[23] P. Finkle, H. D. Draper, and J. H. Hildebrand, J. Am. Chem. Soc. **45**, 2780 (1923).
[24] G. Boniello, C. Blanc, D. Fedorenko, M. Medfai, N. B. Mbarek, M. In, M. Gross, A. Stocco, and M. Nobili, Nat. Mater. **14**, 908 (2015).
[25] A. Dani, G. Keiser, M. Yeganeh, and C. Maldarelli, Langmuir **31**, 13290 (2015).
[26] A. Dörr, S. Hardt, H. Masoud, and H. A. Stone, J. Fluid Mech. **790**, 607 (2016).
[27] K. D. Danov and P. A. Kralchevsky, J. Coll. Int. Sci. **298**, 213 (2006).
[28] A. Einstein, Ann. Phys. **324**, 289 (1906); **339**, 591 (1911).
[29] S. V. Lishchuk, Phys. Rev. E **89**, 043003 (2014).
[30] G. K. Batchelor, *An Introduction to Fluid Dynamics* (Cambridge University Press, Cambridge, 2002).
[31] J. Happel and H. Brenner, *Low Reynolds Number Hydrodynamics* (Prentice Hall, Upper Saddle River, NJ, 1965).
[32] A. W. El-Kareh and T. W. Secomb, Q. J. Mech. Appl. Math. **49**, 179 (1996).
[33] M. Zabarankin and A. F. Ulitko, Q. Appl. Math. **64**, 663 (2006).
[34] M. Zabarankin and P. Krokhmal, Q. J. Mech. Appl. Math. **60**, 99 (2007).
[35] M. Abramowitz and I. A. Stegun (eds.), *Handbook of Mathematical Functions* (National Bureau of Standards, Washington DC, 1972).

[36] F. W. J. Olver, D. W. Lozier, R. F. Boisvert, and C. W. Clark (eds.), *NIST Handbook of Mathematical Functions* (Cambridge University Press, Cambridge, 2010).
[37] J. C. Schneider, M. E. O'Neill, and H. Brenner, Mathematika **20**, 175 (1973).
[38] P. S. Wei and C. Y. Ho, Trans. ASME **73**, 516 (2006).
[39] P. M. Morse and H. Feshbach, *Methods of Theoretical Physics*, Vol. 2 (McGraw–Hill, New York, 1953).
[40] G. A. Korn and T. M. Korn, *Mathematical Handbook* (McGraw–Hill, New York, 1961).
[41] I. N. Sneddon, *The Use of Integral Transforms* (McGraw–Hill, New York, 1972).
[42] M. Galassi, J. Davies, J. Theiler, B. Gough, G. Jungman, P. Alken, M. Booth, and F. Rossi, *GNU Scientific Library Reference Manual* (Network Theory Ltd., Bristol, 2009).
[43] N. Michel and M. V. Stoitsov, Comput. Phys. Commun. **178**, 535 (2008).
[44] A. Gil, J. Segura, and N. M. Temme, Comput. Phys. Commun. **183**, 794 (2012).
[45] H. K. Moffatt, J. Fluid Mech. **18**, 1 (1964).